Investigating the Optimum Carrier Sensing Range Using Transmission Relation Graph in Wireless Ad hoc Networks

Chongqing Zhang
Department of Network Engineering,
Shandong University of Science and Technology, Qingdao, China
gongyouzhang@sina.com

***Abstract*—The size of the carrier sensing range has a great impact on the network performance. Previous studies have focus on computing asymptotic optimum carrier sensing range using unrealistic interference models. In this paper, based on realistic interference model, we propose a framework to determine the optimum carrier sensing range of a network. By regarding the given network and the settings as input and modeling the interferences in wireless networks using transmission relation graph (TRG), our framework can compute a precise optimum carrier sensing range for the given network. Then we use our framework to investigate the changing rules of the optimum carrier sensing range of several types of wireless networks. Simulations are also performed using ns-2, and the results validate the effectiveness of our framework.**

***Index Terms*—carrier sensing range, wireless ad hoc networks, capture effect, transmission relation graph**

I. Introduction

In wireless ad hoc networks, the medium access control (MAC) protocols play a key role in coordinating the access of the shared medium among the nodes [1]. Among the MAC protocols that have been proposed, the IEEE 802.11 protocol is a kind of CSMA/CA (carrier sense multiple access with collision avoidance) MAC protocols and it has been the standard of the wireless LANs. The 802.11 DCF (distributed coordination function) protocol has been also widely studied in the wireless multi-hop ad hoc networks due to its simple implementation and distributed nature. To reduce the collision possibility, it uses carrier sense functions and binary exponential backoff (BEB) mechanism. In particular, two carrier sense functions, physical and virtual carrier-sense functions, are used to determine the state of the medium. The former is provided by the physical layer and the latter by the MAC layer, which uses RTS/CTS handshake to ensure the medium is reserved prior to data packet transmission.

The size of the carrier sensing range (or carrier sensing threshold) has a great impact on the system performance. Although a smaller carrier sensing range (corresponds to a larger carrier sensing threshold) allows more transmissions to happen concurrently, it introduces more interference that may lead failure to more transmissions. On the other hand, a large carrier sensing range (corresponds to a smaller carrier sensing threshold) can protect the transmissions better, but it reduces spatial reuse by only allowing few transmissions to happen concurrently. Therefore, the optimum carrier sensing range should balance the spatial reuse and the impact of collisions so as to optimize the performance of the network.

The problem of evaluating the spatial reuse and finding the optimum carrier sensing range has been studied by a number of recent works [2-10]. However, the interference models of these works are either simplified or ideal. As a result, the optimum carrier sensing ranges computed by these works are still not optimum.

In this paper, based on realistic interference model, we propose a framework that can determine the precise optimum carrier sensing range for any given network. Different from previous studies, our framework regards the network and its settings as inputs. Therefore, our framework is applicable to a network of any topology, no matter the network is dense or sparse, regularly deployed or irregularly deployed. We take capture effect [11] into consideration to compute the optimum carrier sensing range. By introducing transmission relation graph (TRG) to model the interference relations between the transmissions in a wireless ad hoc network, we not only consider the aggregate interference to determine the success or failure of a transmission, but also consider the aggregate signal to judge if a sender can initiate a transmission or not.

The rest of this paper is organized as follows. In Section II, previous studies are reviewed and their interference models are discussed. In Section III, we introduce our framework, including the transmission relation graph (TRG). The results of experiments using our framework and the results of simulations performed using ns-2 are presented in Section IV and Section V respectively. Finally, Section VI concludes this paper.

II. Previous Work

The inefficiency of RTS/CTS mechanism has been addressed in detail in [12]. It is shown in [2, 13] that the

doi:10.4304/jnw.5.4.459-466

spatial reuse efficiency could be improved significantly by tuning the carrier sensing threshold. Based on a simplified interference model, an analytical model is presented in [3, 4] to demonstrate how to derive the optimal sensing threshold given reception power, data rate and network topology. In [5], an experimental testbed based on Intel PRO/Wireless 2200 MiniPCI card is developed to investigate the impact of aggressive carrier sensing threshold on the throughput per user. This paper has noticed the impact of capture effect, but it did not address how to compute the optimum carrier sensing threshold. In [6], Ma et al. presented a Markov model to investigate the effect of the PCS threshold. The interference model adopted in [6] is similar to the interference model in [3, 4].

It is shown in [7] that MAC layer overheads have a great impact on the choice of carrier sensing range. Using similar model as the model in [7], the authors in [8] investigate the impacts of many factors, such as variable transmission ranges and receiver sensitivities for different channel rates, etc, on determining the optimum carrier sensing range. In [9], similar model is adopted to study how to improve spatial reuse through tuning transmit power, carrier sensing threshold and data rate.

The interference model adopted in [3, 4, 6] is shown by Fig. 1. This model only considers the interfering nodes in the interference range, and the interfering nodes outside the range are ignored. However, the aggregate interferences from multiple nodes outside the interference range can be strong enough to wreck the ongoing transmission.

Fig. 2 shows the interference model adopted in [7, 8, 9] to compute the worst case interference that a receiver may receive. The models only consider the receivers whose distance to the sender is equal to the transmission range, and assume the interfering nodes are always available at the desired location whenever they are needed to make it possible for the scheduled transmissions in Fig. 1. However, such a situation rarely happens in practice. First, in a random topology, the possibility that the nodes are located at the desired places is small. Second, even it happens, the chance is still small for all of them successfully contend for the channel for concurrent transmissions. The optimum carrier sensing ranges computed using their network model and worst case interference model are too conservative.

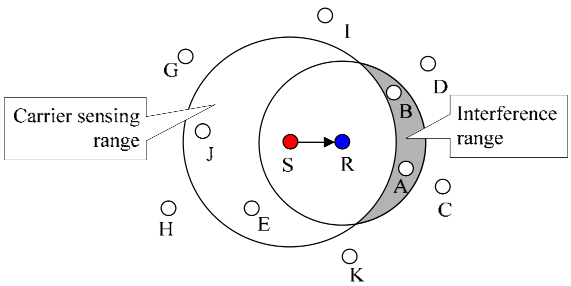

Figure 1. The interference model in [3, 4, 6].

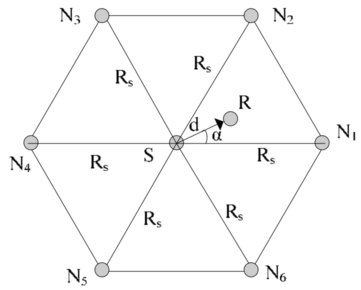

Figure 2. The interference model in [7, 8, 9].

III. The Framework

In this section, the network model and interference model we use are first introduced. Then we propose our framework that includes the metrics, the modeling tool, the algorithm for compute concurrent transmissions set and the algorithm to determine the optimum carrier sensing range.

A. Network Model and Interference Model

In this paper, a wireless ad hoc network is assumed to be composed of a set of homogeneous wireless nodes deployed on a plane. Every node uses an identical transmission power level P^T, which means all nodes have a same transmission range R_t. Every node uses an identical receiving threshold RX_{th}, an identical *SINR* threshold β and an identical carrier sensing threshold CS_{th}. All nodes share a communication channel. The ambient noise strength N is the same all over the network. Radio signal emitted by every node presents the same path loss characteristic.

The radio propagation model used in this paper is given by:

$$P_{ij}{}^{R} = \frac{P_i^T}{d_{ij}{}^{\gamma}} \tag{1}$$

where $P_{ij}{}^R$ is the signal strength of node N_i's transmission as received at node N_j. $P_i{}^T$ is the transmitted power of node N_i, d_{ij} is the distance between N_i and N_j, and γ is the path loss exponent that varies between 2 (free propagation) and 5 (strong attenuation) [14].

In a wireless network, in order for a node N_i to initiate a new transmission to another node, say N_j, the strength of the aggregate signal (including the signals from other nodes and the ambient noise) that node N_i suffers must not exceed the carrier sensing threshold CS_{th}, i.e.,

$$P_i^R = \sum_{k \neq i} P_{ki}^R + N = \sum_{k \neq i} \frac{P_k^T}{d_{ki}{}^{\gamma}} + N \leq CS_{th} \tag{2}$$

where $\sum_{k \neq i} P_{ki}^R$ is the strength of the aggregate signal that node N_i receives from other nodes; and N is the strength of the ambient noise in the network. From equation (2), in order for node N_i to initiate the new transmission, the strength of the aggregate signal it receives from other nodes must be lower than $CS_{th} - N$. Therefore, $CS_{th} - N$ is the upper bound of the strength of the aggregate signal that permits node N_i to initiate the new transmission. In this paper, we call such a threshold the *maximum permissible initiation interference threshold* for transmission from N_i to N_j.

Similarly, in order for a node N_j to correctly receive the transmission from another node, say node N_i, *SINR* of node N_j must exceed the *SINR* threshold β, i.e.,

$$SINR_{ij} = \frac{P_{ij}^R}{\left(\sum_{k \neq i} P_{kj}^R + N\right)} = \frac{P_i^T}{d_{ij}^{\gamma}} \Big/ \left(\sum_{k \neq i} \frac{P_k^T}{d_{kj}^{\gamma}} + N\right) \geq \beta \tag{3}$$

where $\sum_{k \neq i} P_{kj}^R$ is the strength of the aggregate interferences that node N_j receives; and N is the ambient noise in the network. That is, a data packet can be received successfully if its instantaneous signal power is at least β times the instantaneous aggregate interference power. This fact is called *capture effect*. From equation (3), the upper bound of the strength of the aggregate interferences that still allows node N_j to receive successfully is $\frac{P_{ij}^R}{\beta} - N$. In this paper, we call such a threshold the *maximum permissible receive interference threshold* for transmission from N_i to N_j.

B. Performance Metrics

In this paper, following three metrics are used:

1. The number of successful concurrent transmissions in the network. The aggregate throughput of a network depends on both the capacity of every individual transmission link and the total number of successful concurrent transmissions in the network. If the data rate of the shared channel, then the aggregate throughput only depends on the total number of successful concurrent transmissions.
2. The aggregate transmission distance of all successful concurrent transmission. For two networks that have same amount of successful concurrent transmissions, the network with higher aggregate transmission distance has higher spatial reuse performance.
3. The aggregate capacity of all the successful concurrent transmissions. The achievable channel rate r_c of a transmission is calculated by:

$$r_c = W \log_2(1 + SINR) \tag{4}$$

where W is the cannel bandwidth in hertz and *SINR* is the signal to interference and noise ratio.

In order to compute the performance, we need to figure out the concurrent transmissions. When a network is working, the concurrent transmissions in the network vary frequently. We define a set that contains all the allowable concurrent transmissions in a network at a time instant as a *concurrent transmission set*. Note that not all the transmissions in a *concurrent transmission set* are valid, and only the valid transmissions contribute to the aggregate throughput. We define the set that contains all the valid transmissions of a *concurrent transmission set* as a *valid concurrent transmissions set*. As for two *concurrent transmission set*, say CTS_1 and CTS_2, and their corresponding two *valid concurrent transmissions set*, say $VCTS_1$ and $VCTS_2$, $\|CTS_1\| > \|CTS_2\|$ does not mean $\|VCTS_1\| > \|VCTS_2\|$, where $\|CTS_1\|$ is the cardinality of CTS_1.

Only using few *concurrent transmission sets* and *valid concurrent transmissions sets* cannot compute the performance accurately. Suppose we sample the network for a large number of times and get enough number of *concurrent transmission sets* as (CTS_1, CTS_2, …, CTS_n), and the corresponding *valid concurrent transmissions sets* are ($VCTS_1$, $VCTS_2$, …, $VCTS_n$), then the performance is computed using following expression:

$$Performance = \frac{1}{n}\sum_{i=1}^{n} P(VCTS_i) \tag{5}$$

where P($VCTS_i$) is the performance computed by $VCTS_i$.

C. Transmission Relation Graph

A wireless ad hoc network can be modeled as a directed connectivity graph *CG* = (*V*, *E*), where graph vertices and edges represent wireless nodes and *possible transmission links*, respectively. Each member of vertex set $V = (N_1, N_2, \ldots, N_n)$ stands for a wireless node, and an edge (N_i, N_j) is included in edge set *E* if node N_i can communicate with another node N_j directly. Note here for a pair of nodes, say N_i and N_j, that can communicate with each other directly, there are two edge, (N_i, N_j) and (N_j, N_i), are included in set *E*.

To model the interference relations of transmissions in a wireless ad hoc network, we define a transmission relation graph *TRG* = (*T*, *R*), in which the vertices in set *T* correspond to the communication links in the connectivity graph *CG* defined above. The transmission relation graph is similar to the weighted conflict graph proposed in [14]. We use L_{ij} to denote the vertex in set *T* that corresponds to the communication link (N_i, N_j, noise, TH_{init}, I_{init}, TH_{recv}, I_{recv}). In this paper, noise is a constant. TH_{init} and TH_{recv} are computed by following two equations.

$$TH_{init} = CS_{th} - N \tag{6}$$

$$TH_{recv} = \frac{P_{ij}^R}{\beta} - N = \frac{P_i^T}{\beta d_{ij}^{\gamma}} - N \tag{7}$$

The directed edges in set *R* represent the interference relations between communication links. The edge from vertex L_{pq} to L_{ij} has structure as (L_{pq}, L_{ij}, *weight1*, *weight2*), where $i \neq p$, $i \neq q$, $j \neq p$ and $j \neq q$; *weight1* indicates what fraction of the *maximum permissible initiation interferencel* at node N_i is contributed by the activity of communication link L_{pq}. *weight2* indicates what fraction of the *maximum permissible receive* *interference* at node N_j is contributed by the activity of communication link L_{pq}. *weight1* and *weight2* are computed by following two equations:

$$weight1 = \frac{P_{pi}^{R}}{CS_{th} - N} = \frac{\dfrac{P^{T}}{d_{pi}^{\gamma}}}{CS_{th} - N} \quad (8)$$

$$weight2 = \frac{P_{pj}^{R}}{\dfrac{P_{ij}^{R}}{\beta} - N} = \frac{\dfrac{P_{p}^{T}}{d_{pj}^{\gamma}}}{\dfrac{P_{i}^{T}}{\beta d_{ij}^{\gamma}} - N} \quad (9)$$

D. Algorithm

The algorithm for computing the *concurrent transmission sets* runs in cycles and a transmission is chosen to be enabled in each cycle. The repetition continues until every transmission in the transmission relation graph is either enabled or disabled. Given a transmission relation graph *TRG* = (*T*, *R*), we associate a color (*white*, *gray*, or *black*) with each transmission. All transmissions are initially *white* and change color as the algorithm progresses. The algorithm is essentially an iteration of the process of choosing *white* transmissions to dye *gray* or *black*. At the end of the algorithm, every transmission is dyed *gray* or *black*. The black transmissions constitute a maximum concurrent transmission set. The meanings of three colors that a transmission L_{ij} can have are explained as follows:

- *white* – transmission L_{ij} is not in the allowable concurrent transmission set or the disabled transmission set.
- *gray* – transmission L_{ij} is disabled and put into the disabled transmission set.
- *black* – transmission L_{ij} is enabled and put into the allowable concurrent transmission set.

Let T_w, T_b and T_g be the set of *white*, *black* and *gray* transmissions respectively. Initially, all nodes are colored white and included in T_w. T_b and T_g are empty. The algorithm constructs a allowable concurrent transmission set by selecting transmission from T_w. In each step a transmission L_{ij} is chosen to dye *black* is arbitrarily chosen and added to T_b. Then for each transmission L_{pq} still in T_w, the impact of L_{ij} on L_{pq} is added to the aggregate signal of L_{pq}. If the strength of the aggregate signal exceeds the carrier sensing threshold (*aggSignal*(L_{pq}) > 1), then L_{pq} is disabled and added into T_g. The pseudocode of the algorithm is presented by Fig. 3.

The above algorithm is based on saturated networks in which all possible transmissions are selected fairly. By modifying the code of selecting the possible transmission in the algorithm, our framework can easily take routing and other factors that affect the selection of possible transmissions into account.

E. Computing the Optimum Carrier Sensing Range

Given the network and its settings, our framework computes the optimum carrier sensing range using the algorithm shown in Fig. 4.

The changing range of the carrier sensing range is determined by *csrLowBound*, *csrStep* and *csrStepNum*. The carrier sensing rage changes from *csrLowBound* with a step of *csrStep*. For each step, the performance is calculated for each step. The step with the largest performance value is the optimum carrier sensing range.

IV. Experimental Results

The optimum carrier sensing range is affected by many factors, such as transmission power, distribution of nodes, path loss exponent, traffic task, ambient noise, routing protocols, and performance metric, etc. The relation between optimum carrier sensing range and its influencing factors is given in Fig 5. From the figure, the throughput of the network depends on the metric and the happened traffic. Other factors impose their impacts on the throughput by affecting the traffic directly or indirectly.

Therefore, if we know the traffic happened when the network works, then the carrier sensing range can be optimized using the information of the transmissions. And by analyzing how the traffic is affected by the influencing factors, we can know how the carrier sensing range changes with these factors. For this purpose we define traffic distribution map to analyze the relations

```
color each transmission white and add it to T_w;
clear T_b, T_g;
while (T_w is not empty) {
    select an arbitrary transmission L_ij from T_w;
    delete L_ij from T_w;
    add L_ij to T_b;
    for each L_pq in T_w {
        aggSignal(L_pq) += weight(L_ij, L_pq);
        if (aggSignal(L_pq) > 1) {
            color L_pq gray;
            delete L_pq from T_w;
            add L_pq to T_g;
        }
    }
}
```

Figure 3. The algorithm for computing the concurrent transmissions set

```
generate connectivity graph for the network;
generate the transmission relation graph;
double optCSR = 0; double oldP = 0;
for (int i = 0; i < csrStepNum; i++) {
    double csr = csrLowBound + csrStep * i;
    compute concurrent transmissions sets with csr;
    compute valid concurrent transmissions sets;
    compute the performance => p;
    if (p > oldP) optCSR = csr;
}
```

Figure 4. The algorithm for computing optimum CSR

between optimum carrier sensing range and its influencing factors.

In fact, the carrier sensing range also affects the traffic by affecting the number of concurrent transmission in the network. However, as what will be addressed later, it does not affect the possible transmission links and the selection of the possible transmission links, thus the traffic distribution is not dependent on the carrier sensing range.

A. The Traffic Distribution Map

A wireless ad hoc network can be modeled as a directed connectivity graph $CG = (V, E)$, where graph vertices and edges represent wireless nodes and *possible transmission links*, respectively. Each member of vertex set $V = (N_1, N_2, \ldots, N_n)$ stands for a wireless node, and an edge (N_i, N_j) is included in edge set E if node N_i can communicate with another node N_j directly. Note here for a pair of nodes, say N_i and N_j, that can communicate with each other directly, there are two edge, (N_i, N_j) and (N_j, N_i), are included in set E.

We assign two attributes, *anti-interference ability* and *contribution*, to each possible transmission link and use L_{ij} to denote it. Thus such a transmission link L_{ij} can be represented as: L_{ij} = ((N_i, N_j), *anti-interference ability*, *contribution*). The attribution *anti-interference ability* of L_{ij} represents the ability that L_{ij} stands against interference and noise. It depends on the signal power received by the receiver and the ambient noise. Let $A(L_{ij})$ be the *anti-interference ability* of L_{ij}, then $A(L_{ij})$ can be expressed as:

$$A(L_{ij}) = P_{ij}^{\ R} - N = \frac{P_i^T}{d_{ij}^{\ \gamma}} - N \qquad (10)$$

If P_i^T, γ and N are fixed for all transmissions, then the *anti-interference ability* is only dependent on d_{ij}.

The attribution *contribution* of L_{ij} represents how much L_{ij} contributes if it succeeds. It is dependent on the performance metric and can be a constant or a function with transmission distance and carrier sensing range as independent variable.

When a network works, the possible transmission links are selected and scheduled by the routing protocols according to the traffic tasks. The carrier sensing range determines how many of these scheduled transmissions can be activated concurrently in the network. It does not affect the selection of the transmission links.

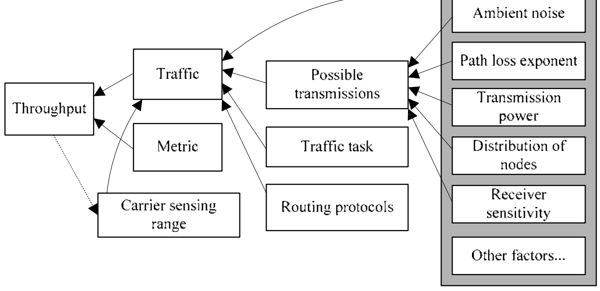

Fig. 5. The influencing factors of optimum carrier sensing range.

For each happened transmission L_{ij} in a long enough time span T, we add a member L_{ij} = ((N_i, N_j), *anti-interference ability*, *contribution*) to a set *TDM*. The traffic distribution map for network *CG* can be defined as:

$$TDM = \{L_1, L_2, \ldots, L_m \mid A(L_i) \geq A(L_{i+1})\} \qquad (11)$$

where $A(L_i)$ is the *anti-interference ability* of L_i. It can be seen the transmissions in a traffic distribution map are listed in descending order by *anti-interference ability*.

The transmissions in the traffic distribution map are selected from the set of possible transmissions. Here we do not consider the impact of traffic tasks and routing protocol, and we will analyze this later. We first consider the networks that are always saturated with transmissions. In such a network a node is always ready to send packets; if a sender judges the channel is idle, it will choose one of its idle neighbors randomly and start a new transmission to the neighbor. Thus every possible transmission is scheduled in a fair way and has the same probability of being selected, and the traffic distribution map is only dependent on the transmission of possible transmissions.

B. Network Types Used in Experiments

Two types of networks shown in Fig. 6 are used in the experiments. The network presented in Fig. 6 (a) is denoted as a *grid* network, and the network presented in Fig. 6 (b) is denoted as a *square* network. Both networks are deployed on square areas. As shown by Fig. 6 (a), we use *inter-node distance* to refer to the distance between a node and one of its instant neighbors in a *grid* network. For a grid network of certain inter-node distance, a corresponding square network of same density is created for comparison.

Every node has a same transmission range of 100 *m*. The path loss exponent is set to be 4. The networks are assumed to be saturated with transmissions, and the algorithm shown in Fig. 3 is adopted to compute the concurrent transmission set. The metrics used are the three metrics addressed above.

Changing Curves of Performance

We first show how the performances change with the carrier sensing range. The networks used are a *grid* network and a *square* network that both are composed of 225 nodes and have a same network area of 525×525 m^2. The inter-node distance of the grid network is 35 *m*.

The performance changing curves of the networks are

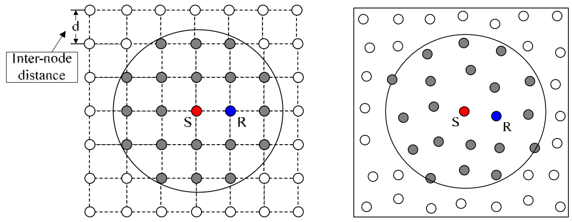

(a) (b)

Figure 6. Two types of networks used in the experiments

presented in Fig. 7 and Fig. 8 respectively. From the figures, it can be observed that the number of transmissions with valid sender is always larger than the number of transmissions with valid receiver. This can be explained by the fact that CSMA mechanism is more efficient in protecting the senders [16].

Optimum Carrier Sensing Ranges of Two Network Types

In this experiment, the grid networks and square networks are also composed of 225 nodes. The inter-node distances of the grid networks range from 30 *m* to 90 *m*. For each grid network, a corresponding square network is generated for comparison.

The results of square networks are presented in Fig. 9. For the square networks, the optimum carrier sensing ranges of three metrics change little with the inter-node distance changes. This can be explained by the fact that different square network have similar traffic distribution maps.

The results of grid networks are presented in Fig. 10. With inter-node distance increases from 30 *m* to 90 *m*, the optimum carrier sensing ranges change drastically. All these changes can be explained by the traffic distribution map. We omit the explanation because of the limitation of paper length.

Optimum Carrier Sensing Range and Density

In this experiment, we have a network area of 400×400 m^2. We increase the number of nodes in the network area so as to create networks of different node densities. Fig. 11 plots how the optimum carrier sensing ranges of two types of network changes with node density. As for the square networks, the optimum carrier sensing ranges fluctuate not much with the node density increases. For the grid networks, the optimum carrier sensing ranges fluctuate drastically when the networks are not dense. Then with the node density increase further, the optimum carrier sensing ranges get close to the optimum carrier sensing ranges of square networks. The explanation of this phenomenon is given in Section IV.

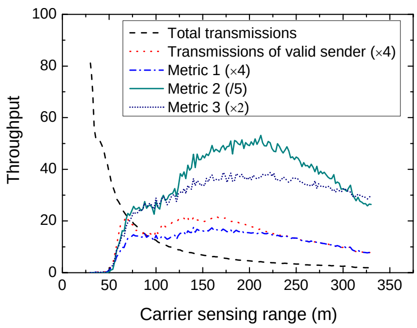

Figure 7. Performance changing curves of a grid network.

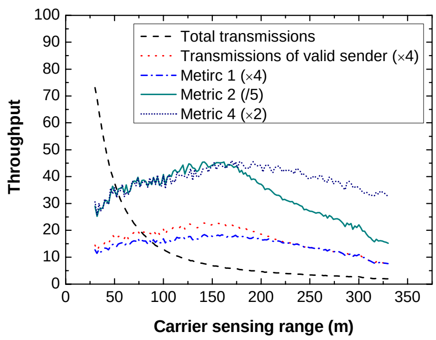

Figure 8. Performance changing curves of a square network.

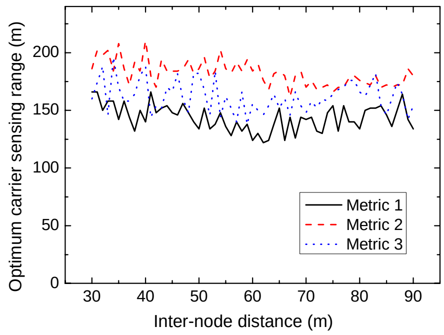

Figure 9. Optimum carrier sensing ranges of square networks.

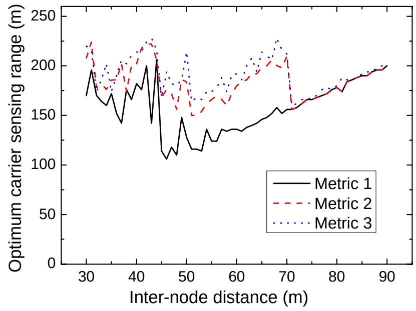

Figure. 10. Optimum carrier sensing ranges of grid networks.

Impact of Path Loss Exponent

We examine how the optimum carrier sensing range changes with path loss exponent using a square network of 225 nodes scattered on an area of 400 × 400 m^2. As Fig. 12 shows, the optimum carrier sensing ranges decreases with the path loss exponent increases.

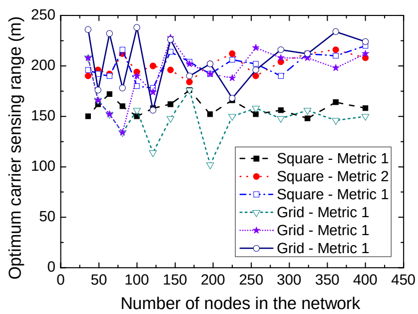

Figure 11. How optimum carrier sensing range changes with node density

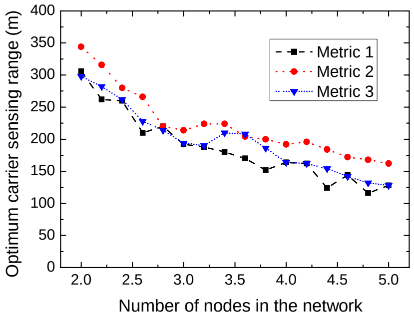

Figure 12. Impact of path loss exponent on optimum carrier sensing range

In [7, 8], it has been observed from the simulation results that the optimum carrier sensing ranges are inclined to be small. It has also been shown in [3, 4] that an aggressive carrier sensing threshold that do not prohibit all the hidden terminals can improve the network throughput. This conclusion also can be observed from the experimental results presented above.

V. Simulation Results

We extend ns-2 to perform our simulations. In the original ns-2 simulator, only transmissions within the carrier sensing range of a receiver are considered as potential sources of collisions. In our extension, all transmissions, including those that are outside the carrier sensing range of a receiver, are considered as interference sources to the receiver. In addition, signals from multiple nodes are also considered when a potential sender senses the carrier signal to judge if the channel is idle or not. When the power of the aggregate signals is higher than the carrier sensing threshold, the channel is considered busy, otherwise the channel is considered idle.

The physical layer characteristics used in the simulation follow the specifications of IEEE 802.11a. The default two-ray radio ground propagation model in ns-2 is used, i.e., the path loss exponent γ = 2 when the distance is less than 86 m and γ = 4 otherwise. The transmit power is set to be 6 dBm. The data rates adopted are 9, 18 and 36 Mbps, and their transmission radii are 119, 178, and 238 *m*.

In the first simulation, three grid networks whose sizes are: 7×7， 10×10 and 12×12 are used. All three networks are deployed on a same area of 1000×1000 m^2. We identify the optimum carrier sensing threshold CS_{th} for one-hop flows. The destination of each packet is chosen randomly from the immediate neighbors of the sender. The data rate is 18 Mbps.

The results are drawn in Fig. 13. From the figure, the optimum carrier sensing thresholds for three networks are -12, -6, and -2 dB respectively. The corresponding carrier sensing ranges of these three thresholds are 340 *m*, 245 *m* and 202 *m* respectively. The inter-node distances of three networks are 143, 100 and 83 *m*. The optimum carrier sensing ranges are approximately $\sqrt[2]{5}$ times of their corresponding inter-node distances. This tallies with the results presented in Fig. 10.

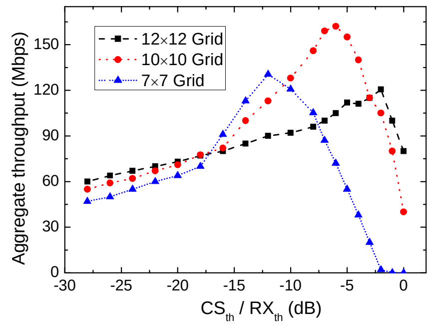

Fig. 13. Optimum carrier sensing threshold of different grid networks.

The second simulation examines the optimum carrier sensing thresholds for different data rates. A 10 × 10 grid network with an area of 1000 × 1000 m^2 is used. The result is shown in Fig. 14. It can be observed from the figure that the higher data rate requires higher SINR and therefore needs a lower carrier sensing threshold (a larger carrier sensing range) to protect the transmissions.

VI. Conclusion

In this paper, based on more realistic network, we propose a framework for computing a precise optimum carrier sensing range for any given network. We also propose a tool, traffic distribution map, to analyze how the optimum carrier sensing range changes with its influencing factors.

Several key observations of this paper are:

Interference model has great impact on the choice of optimum carrier sensing range (or threshold). Unrealistic interference model leads to inaccurate optimum carrier sensing range. The interference model considering the capture effect encourages the optimum carrier sensing ranges to be small.

How the optimum carrier sensing range changes with its influencing factor can be analyzed using traffic distribution map. On the condition that the transmissions are selected and scheduled in a same way, networks with

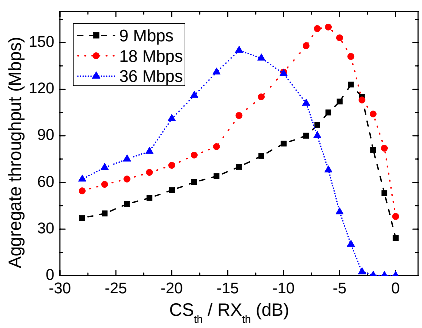

Figure 14. Optimum carrier sensing threshold of different data rates

similar traffic distribution map tend to have similar optimum carrier sensing ranges.

The optimum carrier sensing ranges of randomly deployed networks change little with node density, while the optimum carrier sensing ranges of regularly deployed networks change greatly with node density. A regularly deployed network of high node density tends to have similar optimum carrier sensing range as a randomly deployed network.

REFERENCES

[1] K. Pahlavan and P. Krishnaamurthy, Principles of Wireless Networks, Prentice Hall PTR, New Jersey, 2002.

[2] J. Deng, B. Liang, and P. K. Varshney, "Tuning the carrier sensing range of IEEE 802.11 MAC," GLOBECOM 2004.

[3] J. Zhu, X. Guo, L. L. Yang, and W. S. Conner, "Leveraging Spatial Reuse in 802.11 Mesh Networks with Enhanced Physical Carrier Sensing," ICC 2004.

[4] J. Zhu, et al. "Adaptive Physical Carrier Sensing to maximize spatial reuse in 802.11 mesh networks," Wiley Wireless Communications and Mobile Computing, vol. 4, pp. 933-946, 2004.

[5] J. Zhu, B. Metzler, X. Guo, and York Liu, "Adaptive CSMA for Scalable Network Capacity in High-Density WLAN: a Hardware Prototyping Approach", INFOCOM 2006.

[6] H. Ma, H. M.K. Alazemi, and S. Roy, "A Stochastic Model for Optimizing Physical Carrier Sensing and Spatial Reuse in Wireless Ad Hoc Networks," MASS 2005.

[7] X. Yang and N. H. Vaidya, "On Physical Carrier Sensing in Wireless Ad Hoc Networks," INFOCOM 2005.

[8] H. Zhai and Y. Fang, "Physical Carrier Sensing and Spatial Reuse in Multirate and Multihop Wireless Ad Hoc Networks," INFOCOM 2006.

[9] T. Kim, H. Lim and J. C. Hou, "Improving Spatial Reuse through Tuning Transmit Power, Carrier Sense Threshold, and Data Rate in Multihop Wireless Networks," MOBICOM 2006.

[10] F. Ye and B. Sikdar, "Distance-Aware virtual Carrier Sensing for Improved Spatial Reuse in Wireless Networks," GLOBECOM 2004.

[11] P. Gupta and P. R. Kumar, "The Capacity of Wireless Networks," IEEE Transactions on Information Theory, vol. 46, no. 2, pp. 388-404, March 2000.

[12] K. Xu, M. Gerla, and S. Bae, "How effective is the IEEE 802.11 RTS/CTS handshake in ad hoc networks?" GLOBECOM 2002.

[13] X. Guo, S. Roy, W. Steven Conner, "Spatial Reuse in Wireless Ad-Hoc Networks," VTC 2003.

[14] J. Kivinen, X. Zhao, and P. Vainikainen, "Empirical characterization of wideband indoor radio channel at 5.3 ghz," IEEE trans. on Antenna and Prop., vol. 49, 2001.

[15] K. Jain, J. Padhye, V. Padmanabhan, and L. Qiu, "The impact of interference on multi-hop wireless network performance," MOBICOM 2003.

[16] X. Wang and K. Kar, "Throughput modelling and fairness issues in CSMA/CA based ad-hoc networks," INFOCOM 2005.

Chongqing Zhang joined Shandong University of Science and Technology in July of 2007. He received his Ph.D. in Computer Science from Shanghai Jiaotong University in 2007. He received his master's degree in System Engineering from Xi'an Jiaotong University in 1999. His research interests include performance analysis and protocols design of mobile ad hoc networks and wireless sensor networks.